CO$_2$ Cycloaddition to Epoxides by using M-DABCO Metal–Organic Frameworks and the Influence of the Synthetic Method on Catalytic Reactivity

Bibimaryam Mousavi,[a, b] Somboon Chaemchuen,[a, b] Behrooz Moosavi,[e] Kui Zhou,[a, c] Mekhman Yusubov,[c] and Francis Verpoort*[a, b, c, d]

A series of high-quality M$_2$(BDC)$_2$(DABCO) metal–organic frameworks (abbreviated as M-DABCO; M=Zn, Co, Ni, Cu; BDC= 1,4-benzene dicarboxylate; DABCO=1,4-diazabicyclo[2.2.2]octane), were synthesized by using a solvothermal (SV) method, and their catalytic activity for the cycloaddition of CO$_2$ to epoxides in the absence of a co-catalyst or solvent was demonstrated. Of these metal–organic frameworks (MOFs), Zn-DABCO exhibited very high activity and nearly complete selectivity under moderate reaction conditions. The other members of this MOF series (Co-DABCO, Ni-DABCO, and Cu-DABCO) displayed lower activity in the given sequence. Samples of Zn-DABCO, Co-DABCO, and Ni-DABCO were recycled at least three times without a noticeable loss in catalytic activity. The reaction mechanism can be attributed to structural defects along with the acid–base bifunctional characteristics of these MOFs. Moreover, we illustrate that the synthetic method of M-DABCO influences the yield of the reaction. In addition to the SV method, Zn-DABCO was synthesized by using spray drying due to its industrial attractiveness. It was found that the synthesis procedure clearly influenced the crystal growth and thus the physicochemical properties, such as surface area, pore volume, and gas adsorption, which in turn affected the catalytic performance. The results clarified that although different synthetic methods can produce isostructural MOFs, the application of MOFs, especially as catalysts, strongly depends on the crystal morphology and textural properties and, therefore, on the synthesis method.

1. Introduction

CO$_2$ is a renewable, abundant, inexpensive, and nontoxic source of carbon for the synthesis of fine chemicals and fuels.

[a] Dr. B. Mousavi, Dr. S. Chaemchuen, K. Zhou, Prof. F. Verpoort
Laboratory of Organometallics, Catalysis and Ordered Materials
State Key Laboratory of Advanced Technology for Materials Synthesis and Processing, Wuhan University of Technology, Wuhan 430070 (P.R. China)
E-mail: francis.verpoort@ghent.ac.kr

[b] Dr. B. Mousavi, Dr. S. Chaemchuen, Prof. F. Verpoort
School of Materials Science and Engineering
Wuhan University of Technology, Wuhan 430070 (P.R. China)

[c] K. Zhou, Prof. M. Yusubov, Prof. F. Verpoort
National Research Tomsk Polytechnic University
Lenin Avenue 30, Tomsk 634050 (Russia)

[d] Prof. F. Verpoort
Ghent University, Global Campus
119 Songdomunhwa-Ro, Yeonsu-Gu
Songdo 21985 Incheon (Korea South)

[e] Dr. B. Moosavi
Key Laboratory of Pesticide & Chemical Biology
Ministry of Education, College of Chemistry
Central China Normal University, Wuhan 430079 (P.R. China)

One of the most admired routes for the utilization of CO$_2$ as a C1 building block is through a coupling reaction with epoxides to make five-membered cyclic carbonates; this route is also an essential feature of global carbon management.[1] Cyclic carbonates are known industrially due to their wide applications as organic intermediates, monomers for polymerization, electrolytes in lithium batteries, and aprotic green solvents.[2–6] For this reason, in recent decades, numerous homogeneous and heterogeneous catalysts have been developed by many research groups. The results recommended that the most effective catalysts have both a Lewis acid and a Lewis base or a Lewis acid combined with a nucleophile, which enables them to activate both the epoxide and CO$_2$.[3] However, homogeneous catalysts showed uncompetitive kinetic activity; their limiting factors, such as separation and recovery from solution mixtures, eventually led to a shift towards the development of heterogeneous catalysts instead. Various heterogeneous catalysts, such as zeolites,[7] mesoporous oxides,[8,9] gold nanoparticles supported on resins,[10] and synthetic polymer resins,[11–13] have been reported previously. However, the search for new heterogeneous catalysts with significant properties and high activity that incorporate both acidic and basic sites is still ongoing.

Metal–organic frameworks (MOFs) are a novel class of catalysts with a high surface area (up to 10400 m^{2}g^{-1}), large pore apertures (98 Å), and low density.[14] Their application in numerous syntheses with different metal nodes and linkers, their

ease of functionalization, and the tunability of their particle size and pore volumes are some of the advantages of MOFs over other heterogeneous catalysts.[14–16] Due to these significant properties, to date several MOF structures have been introduced for the conversion of CO_2 to cyclic carbonates. However, MOF catalysts that do not require co-catalysts or cosolvents under mild pressure and temperature for this CO_2 cycloaddition reaction have rarely been reported. In this regard, the M-DABCO MOF series with different metal nodes (M = Ni, Zn, Co, Cu) was synthesized by using the solvothermal method (SV). Their high CO_2 adsorption prompted us to use them as a catalyst for the cycloaddition of CO_2 with epoxides in the absence of any co-catalyst and cosolvent. Their catalytic activity and selectivity were investigated and compared. The most active of the prepared MOFs (Zn-DABCO) was selected and studied in further detail. The aim was to explore the green chemistry precepts of these catalysts, such as chemical stability, reusability, and environmental friendliness. Therefore, Zn-DABCO was synthesized by using the SV and spray-drying (SP) methods. The obtained MOFs were fully characterized and compared with each other as catalysts for the same reaction. To expand the applications of MOFs, the morphology of the crystal should be controlled, which enables studies of the effects of physical and chemical properties on the reactivity of the heterogeneous catalyst. Additionally, the adjustment of MOFs to various applications requires special methods that allow the synthesis of crystals with known sizes and shapes.[16] Accordingly, the synthetic method is one of the most important parameters that can influence the crystal structure and morphology through variations in the crystallization period.[17] With regard to this, Zn-DABCO was synthesized herein by using two different synthetic methods that concomitantly affected the morphology, crystal size, particle shape, pore volume, surface area, and gas adsorption. This simplified our study of the relationship between the structural effects and the application. Both Zn-DABCO samples had similar crystal structures but different topology and, therefore, different physicochemical properties. The variations in these properties were examined by using the catalytic cycloaddition of CO_2 to epichlorohydrin without any additives (e.g., solvents or co-catalysts) as a probe reaction. This independent study shows the effects of the crystal properties of isostructural MOFs on their reactivity, which to the best of our knowledge have hardly been addressed.

2. Results and Discussion

2.1. Catalyst Characterization

M-DABCO MOFs were synthesized according to the reported procedure[18] by using the corresponding metal nitrate salt, 1,4-benzene dicarboxylate (BDC), and 1,4-diazabicyclo[2.2.2]octane (DABCO). The investigation of physical properties was carried out by using X-ray diffraction (XRD), N_2 adsorption–desorption studies, and scanning electron microscopy (SEM). Figure 1 presents the XRD patterns of all M-DABCO samples discussed herein. Based on the IUPAC classification, all M-DABCO MOF
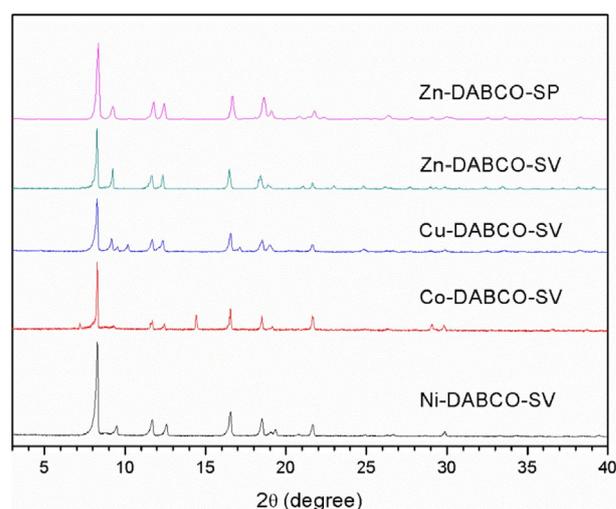
Figure 1. The XRD spectra of the M-DABCO MOF series.

samples exhibited a type I N_2 adsorption–desorption isotherm, which indicated the microporous nature of these materials (Figure S1).[20] Additionally, the surface areas of the M-DABCO MOFs were measured by using Brunauer–Emmett–Teller (BET) and Langmuir methods (see Table S1). The morphology and average size of all crystals were determined by using SEM, and the resulting images are displayed in Figure 2 (Table S1). Leaching of the catalyst after the reaction was investigated by using inductively coupled plasma atomic emission spectroscopy (ICP-AES) to measure the metal content.
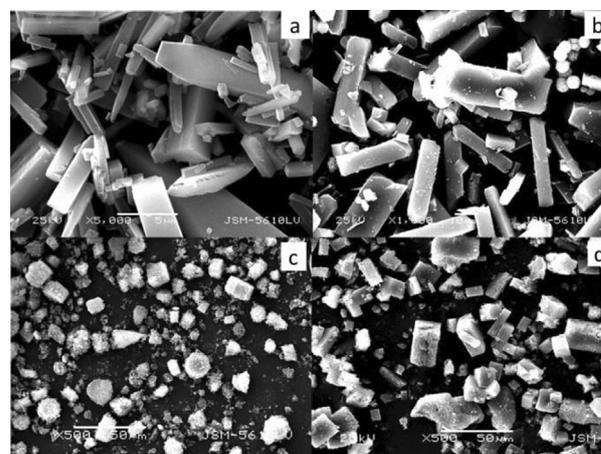
Figure 2. SEM images of a) Ni-DABCO, b) Co-DABCO, c) Cu-DABCO, and d) Zn-DABCO.

2.2. Catalytic Reaction

The catalytic activity of the series of M-DABCO MOFs and isostructural Zn-DABCO (synthesized by the SV or SP method) for the conversion of epoxide to cyclic carbonates was studied and compared. In a typical process, the requisite amount of epoxide and M-DABCO MOF were placed in a 10 mL high-pressure reactor. The reactor was pressurized with CO_2 and was heated to a certain temperature. After reaction completion,

the reactor was cooled to room temperature and the unreacted CO_2 was released. The cyclic carbonate products were then analyzed by using ^1H and ^{13}C NMR spectroscopy.

To find the best reaction conditions, different factors, such as the amount of catalyst, temperature, gas pressure, and reaction duration, were examined for epichlorohydrin by using Zn-DABCO (synthesized by SV) as a model experiment. These conditions were then applied to the other M-DABCO catalysts. Although the CO_2 cycloaddition reaction is known as an exothermic reaction, no significant amount of product was obtained in the absence of any catalyst. The metal salts, DABCO, and BDC linkers were tested individually for their catalytic cycloaddition ability, (Table 1, entries 1–6). As can be seen, in the presence of the metal salt only, the highest achieved yield was as low as 8%. However, in the presence of the DABCO and BDC ligands, conversions of 28 and 14%, respectively, were obtained. Therefore, although these organic compounds (DABCO and BDC) can catalyze this reaction, their catalytic ability is far lower than the catalytic performance of the M-DABCO MOFs. The amount of catalyst (Zn-DABCO) and temperature were the first components to be investigated (Table 1). It was observed that the performance of Zn-DABCO for the CO_2 cycloaddition reaction was improved significantly when the catalyst amount and temperature were increased, and the highest reaction yields were achieved at 100 °C with 100 mg of catalyst (for 18 mmol (1.66 g) epichlorohydrin). The effects of CO_2 pressure and reaction duration were studied next (Table 1), and the temperature and catalyst amount were fixed at the previously determined optimum conditions. An increase in the CO_2 pressure

from 4 to 8 bar improved the conversion from a moderate 62% to almost 100% (Table 1). This is in agreement with the previous report by Han et al.,[21] who demonstrated that an increase in CO_2 pressure led to an enhancement in the solubility of CO_2 in the liquid phase, in which the heterogeneous catalyst is found, which thus resulted in improved epichlorohydrin conversion.

Subsequently, the influence of reaction duration was determined for Zn-DABCO as the catalyst and epichlorohydrin as the substrate (Table 1). At various time periods, a small amount of reaction mixture was filtered and analyzed by using ^1H NMR spectroscopy. The reaction was complete within 12 h at 100 °C and a CO_2 pressure of 8 bar (Figure S2). These results prompted us to apply the same reaction conditions to the other M-DABCO MOFs (Ni, Co, Cu). The outcomes are summarized in Table 1 and are supported by the ^1H NMR spectroscopy results (Figure S3).

Of the different M-DABCO MOFs, Zn-DABCO showed the best performance, that is, the highest conversion combined with almost complete selectivity toward chloropropene carbonate (>99%) without any sign of side products, such as diols or epichlorohydrin dimers. The worst performance was found for Cu-DABCO, which achieved only 18% conversion. The conversion of epichlorohydrin by Ni-DABCO and Co-DABCO for the same reaction were as high as 75 and 86%, respectively. Co-DABCO exhibited acceptably high activity towards the CO_2–epoxide coupling reaction, but the yield of the desired carbonate product was considerably lower than that obtained by using Zn-DABCO (Table 1). To consider why the activities of Zn-DABCO and Co-DABCO are higher than the other MOFs, the acidic properties of the MOFs were tested by using the NH_3-temperature-programmed desorption (TPD) technique (see Table S2 and Figure S9). Obviously, Zn-DABCO and Co-DABCO showed a much higher acidity than Ni-DABCO or Cu-DABCO. The TPD results are in agreement with the catalyst activity of the M-DABCO series in the CO_2 coupling reaction. It should be noted that, of all the reported examples of MOF catalysts for the artificial fixation of CO_2 to epoxides, the most active have Zn or Co as the metal core.[22] Furthermore, according to the TPD analysis, the higher activity of Zn-DABCO compared with Co-DABCO can be explained by the stronger Lewis acidity of Zn compared with Co, which are active sites for this reaction. This is in agreement with the TPD results and also other examples of Zn and Co MOFs reported previously.[22]

Table 2 presents a summary of MOFs reported as catalysts for the cycloaddition of CO_2 to epoxides. MOF-5 (Zn-based MOF) displayed high catalytic performance at low temperature (50 °C) for this cycloaddition reaction.[21] However, to obtain such a high conversion, a quaternary ammonium salt co-catalyst combined with a high pressure of CO_2 (60 bar) are absolutely required. A group of MOFs with different acid–base functionalities were prepared by Kim et al. and screened for the cycloaddition reaction of CO_2 to epoxide.[23] Although some of these MOFs, such as UIO-66 (Zr-based MOF), functionalized UIO-66-NH_2, and MIL-101 (Cr-based MOF), exhibited high activities for this reaction, the performance of the reaction still required both a cosolvent and high pressure (20 bar). Co-MOF-74 is another prototype MOF with excellent catalytic reactivity for the CO_2 cycloaddition reaction, but only in the presence of

Table 1. Conversions and selectivity of the cycloaddition of CO_2 to epoxide under different reaction conditions and with various catalysts (reaction time: 12 h).
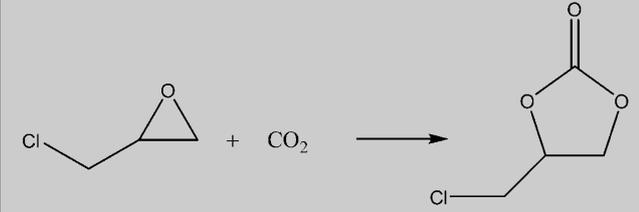
Entry	Catalyst ([mg])	T [°C]	P [bar]	Conversion [%]	Selectivity [%]	Isolated yield [%]
1	$Zn(NO_3)_2 \cdot 6H_2O$	100	8	8	–	–
2	$Ni(NO_3)_2 \cdot 6H_2O$	100	8	5	–	–
3	$Co(NO_3)_2 \cdot 6H_2O$	100	8	6	–	–
4	$Cu(NO_3)_2 \cdot 3H_2O$	100	8	–	–	–
5	H_2BDC	100	8	14	–	–
6	DABCO	100	8	28	–	–
7	Zn-DABCO (60)	100	8	72	99	66
8	Zn-DABCO (80)	100	8	85	99	79
9	Zn-DABCO (100)	100	8	>99	99	97
10	Zn-DABCO (100)	60	8	30	96	21
11	Zn-DABCO (100)	80	8	75	99	71
12	Zn-DABCO (100)	90	8	92	99	88
13	Zn-DABCO (100)	100	4	62	97	55
14	Zn-DABCO (100)	100	6	87	99	75
15	Cu-DABCO (100)	100	8	18	97	13
16	Ni-DABCO (100)	100	8	75	99	71
17	Co-DABCO (100)	100	8	86	78	65

Table 2. Comparison of reaction conditions (temperature and pressure) and performance of Zn-DABCO with the reported MOFs for the cycloaddition of CO_2 to epichlorohydrin.

Catalyst	T [°C]	P [bar]	Conversion [%]	Selectivity [%]	Ref.
ZIF-90[a]	120	11.7	43	–	[28]
F-ZIF-90[a]	120	11.7	96.6	≈100	[28]
UIO-66[b]	100	20	94	–	[23]
UIO-66-NH$_2$[b]	100	20	95	≈100	[23]
ZIF-67[c]	95	8	99	≈100	[26]
MOF-5[d]	50	60	97.6	–	[21]
MIL-101[e]	100	20	63	–	[23]
Co-MOF-74[f]	100	20	96	≈100	[24]
ZIF-8[g]	100	7	98	33	[25]
ZIF-68[h]	120	10	93	≈100	[27]
Zn-DABCO	100	8	>99	≈100	this work

[a] Substrate = epichlorohydrin, 6 h reaction time. [b] Styrene oxide, with cosolvent, 4 h. [c] Epichlorohydrin, 8 h. [d] Styrene oxide, with nBu$_4$NBr co-catalyst and cosolvent, 4 h. [e] Styrene oxide, with cosolvent, 4 h [f] Styrene oxide, with cosolvent, 4 h. [g] Epichlorohydrin, 4 h. [h] Styrene oxide, 12 h.

chlorobenzene as a co-solvent.[24] In contrast to all the other examples (see Table 2), Zn-DABCO catalyzed this coupling reaction in the absence of any solvent or co-catalyst.

Recently, ZIF-8 (Zn-based)[25] and ZIF-67 (Co-based)[22, 26] MOFs were introduced as very active catalysts for the cycloaddition of CO_2 to epichlorohydrin without the need for co-solvents and co-catalysts. Both catalysts were synthesized and compared with Zn-DABCO. In agreement with previous reports, the reaction duration with ZIF-8 was very short (4 h), but its selectivity towards the desired cyclic carbonates was as low as 33.4 % due to polymerization and dimer/diol formation. In contrast, Zn-DABCO showed almost complete selectivity towards the carbonate product.

In addition to MOF-type catalysts, there are other sustainable solid catalysts for CO_2/epoxide coupling, such as polymeric ionic liquids (ILs), conjugated microporous polymers (CMPs), polyamine, and functionalized ion-exchange resins.[39] In general, to date almost all reported polymeric ILs and polyamines[39–42] have demonstrated appreciable catalytic activity, but at higher temperature (> 110) and CO_2 pressure (40–50 bar). The development of coordinated CMPs with a high adsorption capacity for CO_2 made them high-value applicants for CO_2 reactions. Of these compounds, a class of cobalt/aluminum CMPs[43–45] showed very high catalytic performance at room temperature and ambient pressure of CO_2, but mostly in the presence of a co-catalyst. In contrast, Zn-DABCO MOF can function without solvents and co-catalysts under moderate conditions. Additionally, the convenient synthesis of the Zn-DABCO MOF and its ease of handling make it a suitable alternative candidate.

2.3. Recycling Study

The reusability of the heterogeneous M-DABCO series is an important issue and was considered in this study. After the reaction, the catalyst was isolated by centrifugation, washed three

times with DMF, and dried at 80 °C for 12 h under reduced pressure before reuse. Samples of Zn-DABCO, Ni-DABCO, and Co-DABCO were reused at least three times without a perceptible loss in catalytic activity. The recycling behavior of Cu-DABCO was not explored because its activity was very low. The XRD spectra of the catalysts after the third catalytic cycle are displayed in Figure S4, and show that the crystalline structures were preserved even after three cycles. An X-ray photoelectron spectroscopy (XPS) study of the MOFs was carried out to gain information on the oxidation state of the metal nodes after the reaction (Figure S5). The XPS results revealed that the oxidation state of the reused MOFs did not change compared with fresh samples, and corresponded to Zn^{II}, Ni^{II}, and Co^{II}. These results are in agreement with the XRD results and confirm that the crystalline structure of the M-DABCO MOFs was preserved after three cycles. This is consistent with the findings of Nguyen, Phan et al.[29, 30] who reported the reusability potential of M-DABCO MOFs in other organic reactions. Subsequently, after the third use, the filtrate solution of the reaction mixture with the most active catalyst (Zn-DABCO) was analyzed by using ICP-AES, and just less than 0.1 wt % Zn was found in the solution, which indicated the structural stability of Zn-DABCO. For the other MOFs (Co-DABCO and Ni-DABCO) 0.2 and 0.15 wt % Co and Ni was found, respectively. Additionally, a hot filtration test was performed for each M-DABCO catalyst, which revealed that no activity was detected in the filtrate after filtration and, therefore, the small amount of leached metal was not catalytically active for the reaction. Subsequently, to determine the usefulness of these catalysts, the most reactive catalyst (Zn-DABCO-SV) was selected and applied for the CO_2 cycloaddition reaction with different epoxides. Table 3 lists the results and the ^{1}H NMR spectra are illustrated in the Supporting Information. The reaction conditions were altered for various epoxides depending on the size of the molecules; apparently larger molecules needed a longer time to diffuse through the MOFs.

Table 3. Various epoxides catalyzed by using Zn-DABCO in the absence of solvent and co-catalyst.

Epoxide	t [h]	T [°C]	Conversion [%]
propylene oxide	18	100	96
styrene oxide	30	110	90
2-(phenoxymethyl)oxirane	25	100	92
epichlorohydrin	12	100	>99

2.4. The Effect of the Synthetic Method on Morphology and Reactivity

Zn-DABCO, synthesized by using two different synthetic techniques, was used to assess the different physical and chemical properties with respect to the crystal structure and topology. The two catalysts were employed for the first time for the CO_2 cycloaddition of epoxides. Surprisingly, it was found that their activity as catalysts was very different. This prompted us to investigate their physicochemical properties and their relation-

ship to the corresponding synthetic methods. Recently, several studies have focused on the investigation of isoreticular MOFs with special properties for the evaluation of different physical and/or chemical parameters.[31–34] For example, isoreticular ZIFs were used to clarify the relationship between the BET surface area and gas adsorption.[32] In another work, the effect of particle size on the adsorption kinetics was investigated for isoreticular MOFs.[34] These studies are particularly significant to increase the knowledge of morphology and crystal-size control in MOFs, which influences the physicochemical properties and thus their potential applications.[35] From the obtained results, it is clear that Zn-DABCO is the most active catalyst of the presented M-DABCO MOFs and thus Zn-DABCO MOF was selected to be synthesized by using another synthetic method. Herein, the SP method was applied as an alternative to the SV method, and gave Zn-DABCO-SP with a different crystal morphology. More information on the crystal structures was obtained by using powder X-ray diffraction (Figure 1). Undoubtedly, the XRD pattern of Zn-DABCO-SP is similar to the XRD pattern of Zn-DABCO-SV, which implies that both catalysts are isostructural. Notably, the XRD patterns are completely reproducible and comparable to the simulated structure. Although both Zn-DABCO-SV and -SP present very similar XRD patterns, their morphological features and average crystal sizes are completely distinct. The SEM images of Zn-DABCO-SP (Figure S6) and Zn-DABCO-SV (Figure 2d) conspicuously indicate their distinctive crystal morphology, shape, and size. Specifically, Zn-DABCO-SV crystallites showed a rectangular shape with an average size of 25 μm, whereas Zn-DABCO-SP crystallites exhibited small rod-shaped crystals with a size of less than 1 μm. It should be noted that both Zn-DABCO samples (SP and SV) were synthesized by using the optimal conditions reported in the literature and the effects of other features, such as the solvent and the ratio of ligands to metal ions, were neglected.

As shown in Figure S1, the N_2 adsorption isotherm is type I, which suggests a microporous nature for Zn-DABCO-SP. The BET and Langmuir methods were performed to assess the surface area, porosity properties, and CO_2 adsorption (summarized in Table S1). These variations in the physicochemical properties were studied through the catalytic fixation of CO_2 to epichlorohydrin. As mentioned above, this enabled a direct analysis of the effects of the crystal properties of the Zn-DABCO MOFs on the reactivity for this coupling reaction. The optimal reaction conditions, described above for Zn-DABCO-SV, were applied to Zn-DABCO-SP. However, the reaction was stopped after 7 h, before completion, to ascertain the magnitude of the difference between the two catalysts. The catalysts were then separated by using centrifugation and the final product and the reaction conversion to carbonates were analyzed by using ^1H NMR spectroscopy (Figure S7). The reaction was repeated three times for each Zn-DABCO sample and similar results were obtained each time.

According to the results, Zn-DABCO synthesized by using the SV method exhibited a conversion of more than 50% in 7 h, which was more than 17% higher than the conversion obtained by using Zn-DABCO-SP. The textural properties, such as pore size, volume, surface area, and CO_2 adsorption for both

Zn-DABCO samples were compared and the results are depicted in Table S1. Evidently there is a relation between the conversion and the textural properties. The surface area and pore volume of Zn-DABCO-SV were higher than the surface area and pore volume of Zn-DABCO-SP. This indicates that a higher surface area and pore volume in Zn-DABCO-SV delivers more active sites for the reaction, which eventually leads to increased reactivity. In contrast, Zn-DABCO-SP, with a lower surface area and pore volume, displayed limited reactivity. These results are in agreement with previous reports that include analytical and DFT calculations for MOFs as catalysts, which confirms that the active sites of MOFs are located on the external surface or in defects.[22, 37] Another important textural property is gas adsorption, particularly herein. CO_2 is one of the substrates and a higher gas adsorption directly influences the reactivity of the catalyst. As shown in Table S1, the higher CO_2 adsorption of Zn-DABCO-SV (101 cm^3 g^{-1}) compared with that of Zn-DABCO-SP (87 cm^3 g^{-1}) affected the reactivity for this reaction in the same sequence. Although one could expect that the smaller particle size of Zn-DABCO-SP would result in a lower diffusion limit and higher reactivity, Zn-DABCO-SV, with a bigger particle size, showed better catalytic performance. This could occur because the effect of surface area, pore volume, and CO_2 adsorption is more effective than particle size specifically for small reactant molecules, which is in agreement with a previous study of the effects of particle size on the reactivity of MOFs, reported by Corma et al.[46]

2.5. Catalyst Mechanism

The mechanism for the artificial fixation of CO_2 to epoxides has been described in the literature.[25] As mentioned earlier, the most effective catalysts have both Lewis acid and Lewis base sites. For example, previous studies have shown that catalysts such as zeolites or mesoporous silicate with acid–base pairs are more active.[38] The catalytic sites of MOFs for the CO_2/epoxides coupling reaction may be the nodes/secondary building units (SBU), the functional linkers, or both.[38] The DABCO-MOFs have saturated nodes that are linked to two different ligands; BDC and DABCO. Although the metal nodes in M-DABCO MOF are coordinatively saturated, as in ZIF-8, ZIF-67, or MOF-5, the transformation reaction can be catalyzed by structural defects and/or defects on the surface.[25] Therefore, the catalytic activity is related to the amount of defects because structural defects can show acid and/or basic properties, which in turn influence the reactivity of the MOF as a catalyst. Therefore, a TPD study was performed by using NH_3 (NH_3-TPD) and CO_2 (CO_2-TPD) as probe gas molecules to evaluate the acidic and basic sites, respectively. Figure S9 and Table S2 present the TPD results for the M-DABCO series. The results of the NH_3-TPD study gave the approximate value of acid sites (unsaturated metal nodes), which mainly confirmed the presence of unsaturated metal active sites. Another important approach that should be considered in the catalysis mechanism of DABCO MOFs is the DABCO linker. If the organic linkers can act similarly to a co-catalyst to activate CO_2, the MOF catalyst would be more efficient. In addition, it is known that amines have a high

affinity for CO_2, and the DABCO ligand in this series of MOFs is a highly nucleophilic amine.[25] Although DABCO linkers are mostly coordinated in the frameworks,[18] there are also some uncoordinated DABCO ligands present at defects and/or on the surface that can act as basic active sites. Moreover, the CO_2-TPD results (Figure S10) clearly demonstrate the presence of basic sites in the DABCO MOF series. The role of the DABCO linker was clarified further when the activity of Zn-DABCO MOF was compared with the activity of MOF-5 for the same reaction.[21] MOF-5 has coordinatively saturated metal centers (Zn) in the node with unfunctionalized BDC linkers, whereas the Zn-DABCO MOF has the same metal nodes and linker plus the DABCO linker. Due to the lack of basic sites in MOF-5, tetraalkylammonium halide is required as a co-catalyst[21] for the CO_2/epoxide coupling, whereas the Zn-DABCO MOF catalyzed the cycloaddition reaction in the absence of any co-catalyst. Moreover, for this reaction, MOF-5 required a CO_2 pressure of up to 20 bar, whereas in the presence of amine linkers, as in Zn-DABCO, only 8 bar of CO_2 was needed. Therefore, the uncoordinated DABCO linkers in Zn-DABCO act as Lewis bases (Figure 3). Moreover, it was presumed herein that the N moieties of uncoordinated DABCO linkers have reasonable Lewis basicity, which favors the binding and activation of CO_2. Additionally, the micropores of the DABCO-MOFs do not restrict the entrance of substrates into the cavities. Therefore, catalysis can occur on both the exterior and interior of the crystallites.
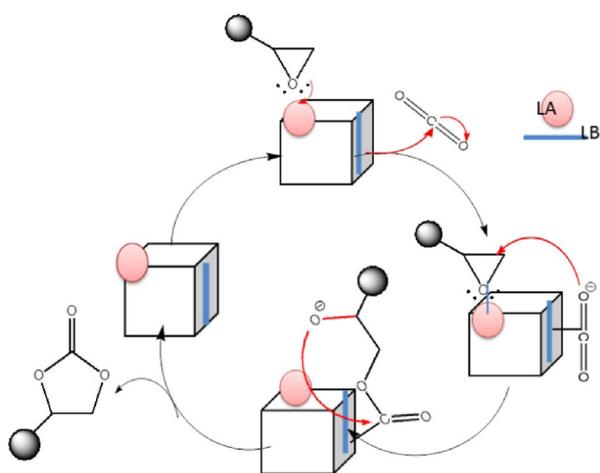
Figure 3. A possible mechanism for the cycloaddition of CO_2 to epoxide by using the Zn-DABCO catalyst; LA = Lewis acid and LB = Lewis base.

3. Conclusions

Herein, four different M-DABCO MOFs (M = Zn, Co, Ni, Cu) were synthesized by using a SV method and were applied as new catalysts for the cycloaddition of CO_2 to epoxides in the absence of any solvent or co-catalyst. It was confirmed that, according the TPD results, the sequence of activity was in agreement with the MOF acidic properties. Of the prepared MOFs, Zn-DABCO showed a very high activity and virtually 100% selectivity. Moreover, Zn-DABCO exhibited very high activity comparable to or better than previously reported MOF catalysts for

this reaction. Subsequently the influence of the synthetic method (SV or SP) on the catalytic performance of Zn-DABCO was investigated. It was discovered that the synthetic method certainly affects the crystal structure and morphology and, consequently, the surface area, porosity, and gas adsorption. The changes in these physicochemical properties in turn influenced the catalytic reactivity. This work illustrates that although different synthetic methods can produce isostructural MOFs with identical XRD patterns, the applicability of the MOFs, particularly as catalysts, strongly depends on the crystal morphology and textural properties.

Experimental Section

Materials and Methods

All starting materials and solvents were obtained from commercial sources and used as received.

Catalyst Preparation

M-DABCO MOFs (M = Zn, Co, Cu, Ni) were synthesized from the metal nitrate salt, 1,4-benzene dicarboxylate (BDC), and 1,4-diazabicyclo[2.2.2]octane (DABCO) ligands, as described in previous reports.[18] Zn-DABCO-SP was synthesized according to the method reported by Carné-Sánchez et al.[19] by using an AF-88 labs Spray dryer (AFIND Scientific Instrument Co.). In this procedure, two solutions of zinc nitrate hexahydrate (0.362 g) and terephthalic acid (0.415 g) in DMF (15 mL) were prepared. These two solutions were combined with a solution of 1,4-diazabicyclo[2.2.2]octane (0.140 g) in DMF (15 mL). The mixture was then shaken for 2 min and then supplied to the spray-dryer (spray nozzle 8 mm) at a rate of 300 mL h^{-1} (flow rate 160 m^3 h^{-1}) and an inlet temperature of 180 °C. The white powder was recovered and washed three times with DMF. The wet product was dried at 25 °C under reduced pressure for 12 h.

Catalytic Reaction

All cycloaddition reactions were performed in a 10 mL stainless-steel high-pressure reactor (XINGDA, Beijing, China). In a standard reaction, the MOF catalyst (100 mg) and the epoxide (18 mmol) were placed in the batch reactor and pressurized with CO_2. Reactions were conducted at different temperatures, CO_2 pressures, and reaction times to obtain the optimum conditions. After reaction completion, the reactor was cooled to RT, then gradually depressurized. Subsequently, the catalyst was filtered off and the final product was identified by using ^{1}H NMR spectroscopy. To test the recyclability of the catalyst, the catalyst was recovered by centrifugation and washed three times with DMF. The catalyst was then dried under reduced pressure at 80 °C for 12 h, after which it was ready for a new cycle.

Characterization Methods

The TGA studies of M-DABCO MOFs were carried out by using a Netzsch STA 409 apparatus under an N_2 atmosphere. The XRD patterns were collected by using a Bruker D8 advance diffractometer (Bragg–Brentano geometry) at 40 kV and 45 Ma with $Cu_{K\alpha}$ radiation and a scanning rate of 6° min^{-1}. The pore-size distribution and adsorption–desorption isotherms were measured by using a Micro-

Acknowledgements

Conflict of Interest

The authors declare no conflict of interest.

[1] W. Keim (Ed.), *Catalysis in C1 Chemistry*, D. Reidel Publishing Company **2012**.

[2] T. Sakakura, J. C. Choi, H. Yasuda, *Chem. Rev.* **2007**, *107*, 2365–2387.

[3] M. North, R. Pasquale, C. Young, *Green Chem.* **2010**, *12*, 1514–1539.

[4] Y. Zhou, S. Hu, X. Ma, S. Liang, T. Jiang, B. Han, *J. Mol. Catal. A* **2008**, *284*, 52–57.

[5] A. A. G. Shaikh, S. Sivaram, *Chem. Rev.* **1996**, *96*, 951–976.

[6] N. Kielland, C. J. Whiteoak, A. W. Kleij, *Adv. Synth. Catal.* **2013**, *355*, 2115–2138.

[7] C. G. Li, L. Xu, P. Wu, H. Wu, M. He, *Chem. Commun.* **2014**, *50*, 15764–15767.

[8] K. Yamaguchi, K. Ebitani, T. Yoshida, H. Yoshida, K. Kaneda, *J. Am. Chem. Soc.* **1999**, *121*, 4526–4527.

[9] R. Srivastava, D. Srinivas, P. Ratnasamy, *Tetrahedron Lett.* **2006**, *47*, 4213–4217.

[10] F. Shi, Q. Zhang, Y. Ma, Y. He, Y. Deng, *J. Am. Chem. Soc.* **2005**, *127*, 4182–4183.

[11] C. Qi, J. Ye, W. Zeng, H. Jiang, *Adv. Synth. Catal.* **2010**, *352*, 1925–1933.

[12] Y. Xie, Z. Zhang, T. Jiang, J. He, B. Han, T. Wu, K. Ding, *Angew. Chem. Int. Ed.* **2007**, *46*, 7255–7258; *Angew. Chem.* **2007**, *119*, 7393–7396.

[13] C. Kohrt, T. Werner, *ChemSusChem* **2015**, *8*, 2031–2034.

[14] H. Deng, S. Grunder, K. E. Cordova, C. Valente, H. Furukawa, M. Hmadeh, F. Gándara, A. C. Whalley, Z. Liu, S. Asahina, *Science* **2012**, *336*, 1018–1023.

[15] O. K. Farha, I. Eryazici, N. C. Jeong, B. G. Hauser, C. E. Wilmer, A. A. Sarjeant, R. Q. Snurr, S. T. Nguyen, A. O. Yazaydın, J. T. Hupp, *J. Am. Chem. Soc.* **2012**, *134*, 15016–15021.

[16] J. Cravillon, S. Münzer, S. J. Lohmeier, A. Feldhoff, K. Huber, M. Wiebcke, *Chem. Mater.* **2009**, *21*, 1410–1412.

[17] A. Schejn, L. Balan, V. Falk, L. Aranda, G. Medjahdi, R. Schneider, *CrystEngComm* **2014**, *16*, 4493–4500.

[18] S. Chaemchuen, K. Zhou, N. A. Kabir, Y. Chen, X. Ke, G. Van Tendeloo, F. Verpoort, *Microporous Mesoporous Mater.* **2015**, *201*, 277–285.

[19] A. Carné-Sánchez, I. Imaz, M. Cano-Sarabia, D. Maspoch, *Nat. Chem.* **2013**, *5*, 203–211.

[20] K. S. Sing, *Pure Appl. Chem.* **1985**, *57*, 603–619.

[21] J. Song, Z. Zhang, S. Hu, T. Wu, T. Jiang, B. Han, *Green Chem.* **2009**, *11*, 1031–1036.

[22] R. R. Kuruppathparambil, T. Jose, R. Babu, G. Y. Hwang, A. C. Kathalikkattil, D. W. Kim, D. W. Park, *Appl. Catal. B* **2016**, *182*, 562–569.

[23] J. Kim, S. N. Kim, H. G. Jang, G. Seo, W. S. Ahn, *Appl. Catal. A* **2013**, *453*, 175–180.

[24] H. Y. Cho, D. A. Yang, J. Kim, S. Y. Jeong, W. S. Ahn, *Catal. today* **2012**, *185*, 35–40.

[25] C. M. Miralda, E. E. Macias, M. Zhu, P. Ratnasamy, M. A. Carreon, *ACS Catalysis* **2011**, *2*, 180–183.

[26] B. Mousavi, S. Chaemchuen, B. Moosavi, Z. Luo, N. Gholampour, F. Verpoort, *New J. Chem.* **2016**, *40*, 5170–5176.

[27] L. Yang, L. Yu, G. Diao, M. Sun, G. Cheng, S. Chen, *J. Mol. Catal. A* **2014**, *392*, 278–283.

[28] T. Jose, Y. Hwang, D. W. Kim, M. I. Kim, D. W. Park, *Catal. Today* **2015**, *245*, 61–67.

[29] T. Truong, C. K. Nguyen, T. V. Tran, T. T. Nguyena, N. T. S. Phan, *Catal. Sci. Technol.* **2014**, *4*, 1276–1285.

[30] T. N. Tu, K. D. Nguyen, T. N. Nguyen, T. Truong, N. T. S. Phan, *Catal. Sci. Technol.* **2016**, *6*, 1384–1392.

[31] Y. Houndonougbo, C. Signer, N. He, W. Morris, H. Furukawa, K. G. Ray, D. L. Olmsted, M. Asta, B. B. Laird, O. M. Yaghi, *J. Phys. Chem. C* **2013**, *117*, 10326–10335.

[32] W. Morris, B. Leung, H. Furukawa, O. K. Yaghi, N. He, H. Hayashi, Y. Houndonougbo, M. Asta, B. B. Laird, O. M. Yaghi, *J. Am. Chem. Soc.* **2010**, *132*, 11006–11008.

[33] M. Eddaoudi, H. Li, O. M. Yaghi, *J. Am. Chem. Soc.* **2000**, *122*, 1391–1397.

[34] X. Fan, J. Zhou, T. Wang, J. Zheng, X. Li, *RSC Adv.* **2015**, *5*, 58595–58599.

[35] J. Zakzeski, A. Dębczak, P. C. A. Bruijnincx, B. M. Weckhuysen, *Appl. Catal. A* **2011**, *394*, 79–85.

[36] J. Lee, O. K. Farha, J. Roberts, K. A. Scheidt, S. T. Nguyen, J. T. Hupp, *Chem. Soc. Rev.* **2009**, *38*, 1450–1459.

[37] C. Chizallet, S. Lazare, D. Bazer-Bachi, F. Bonnier, V. Lecocq, E. Soyer, A. A. Quoineaud, N. Bats, *J. Am. Chem. Soc.* **2010**, *132*, 12365–12377.

[38] M. H. Beyzavi, C. J. Stephenson, Y. Liu, O. Karagiaridi, J. T. Hupp, O. K. Farha, *Front. Energy Res.* **2015**, *2*, 63.

[39] X. D. Lang, X. F. Liu, L. N. He, *Current Organic Chemistry* **2015**, *19*, 681–694.

[40] M. F. Rojas, F. L. Bernard, A. Aquino, J. Borges, F. D. Vecchia, S. Menezes, R. Ligabue, S. Einloft, *J. Mol. Catal. A* **2014**, *392*, 83–88.

[41] J. Eastoe, S. Gold, D. C. Steytler, *Langmuir* **2006**, *22*, 9832–9842.

[42] J. L. He, T. B. Wu, Z. F. Zhang, K. L. Ding, B. X. Han, Y. Xie, T. Jiang, Z. M. Liu, *Chem. Eur. J.* **2007**, *13*, 6992–6997.

[43] Y. Xie, T. T. Wang, R. X. Yang, N. Y. Huang, K. Zou, W. Q. Deng, *ChemSusChem* **2014**, *7*, 2110–2114.

[44] Y. Xie, T. T. Wang, X. H. Liu, K. Zou, W. Q. Deng, *Nat. Commun.* **2013**, *4*, 1960–1967.

[45] Y. Xie, R. X. Yang, N. Y. Huang, H. J. Luo, W. Q. Deng, *J. Energy Chem.* **2014**, *23*, 22–28.

[46] A. Dhakshinamoorthy, M. Alvaro, Y. K. Hwang, Y. K. Seo, A. Corma, H. Garcia, *Dalton Trans.* **2011**, *40*, 10719–10724.